Dynamics of Diffraction Dissociation

V.A. Khoze, A.D.Martin, M.G. Ryskin (EPJ C81,175)

$$\Psi = \Phi(R)\psi(r_i)$$

Diffraction - the process where the internal wave function $\psi(r_i)$ is not destroyed.

Elastic scattering is caused by the absorption of part of $\Phi(R)$

Good-Walker formalism

To describe the low mass
$p \to N^*$, $N_a^* \to N_b^*$ **transitions**

$$\langle \phi_i | T | \phi_k \rangle = 0 \qquad \text{for } i \neq k \qquad |i\rangle = \sum_k a_{ik} \, |\phi_k\rangle$$

After the interaction we get
another **coefficients** a'_{ik} **and**
thus the ***new*** **states are generated**

$$\pi + A \to jj + A$$

from small size $q\bar{q}$ **component of** π

$$\sigma(q\bar{q}) \propto \alpha_s^2 < r^2 >$$

High-mass diffractive dissociation

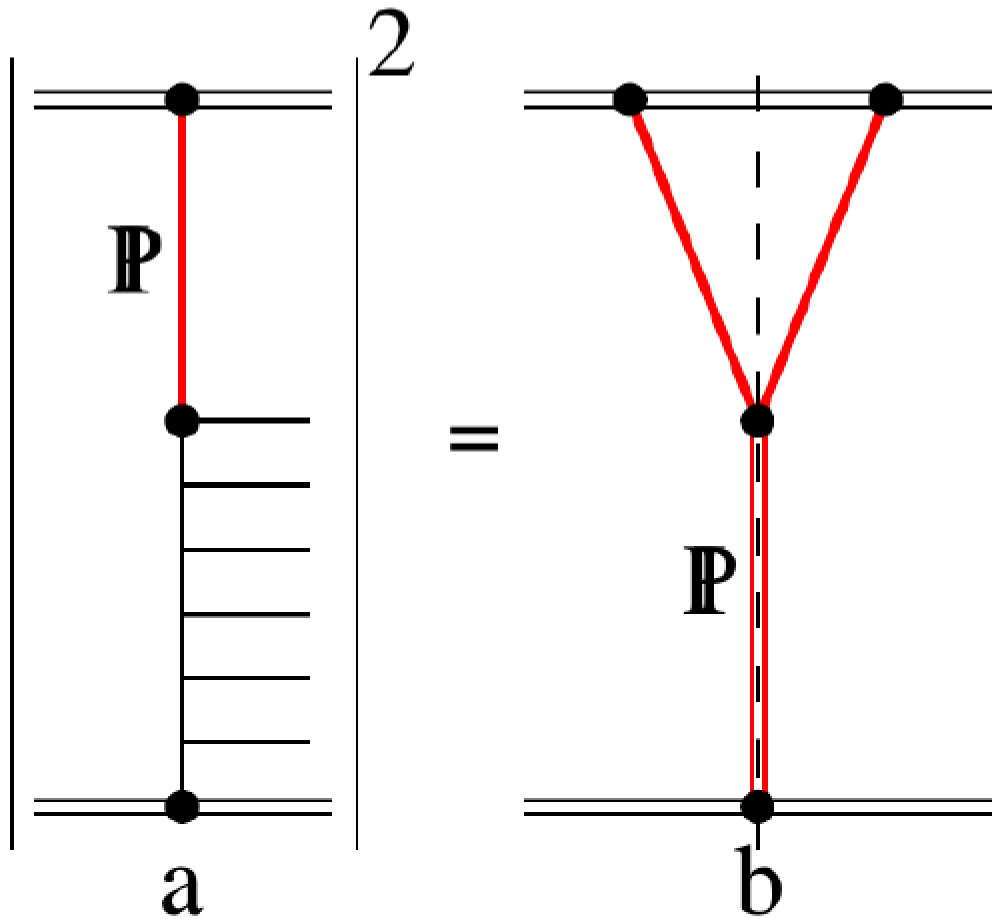

$$\Psi \;=\; \Phi(R)\psi(r_i)$$

Diffractive dissociation – the low x partons from $\psi(r_i)$ save its coherence

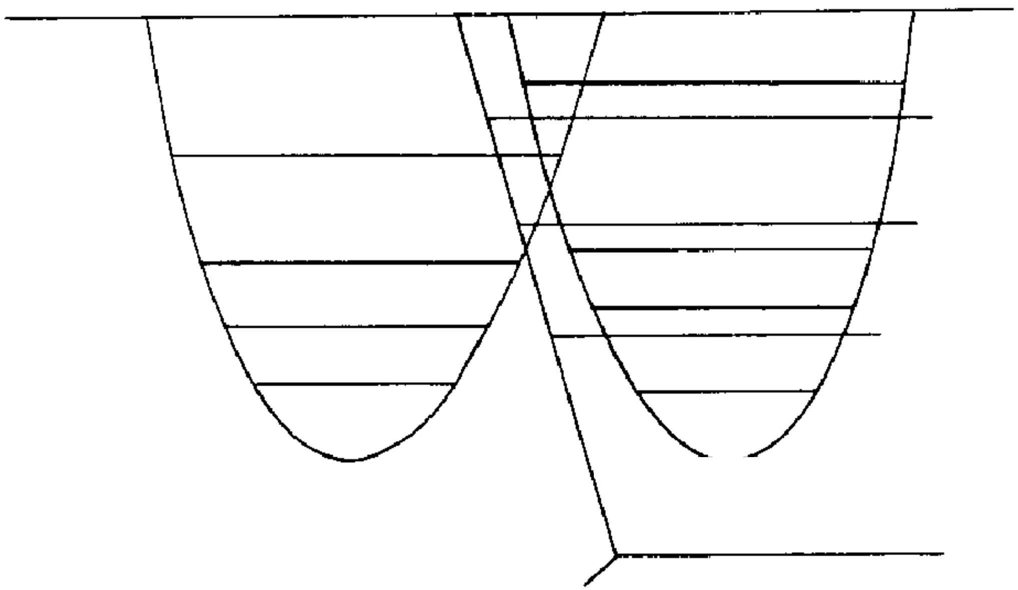

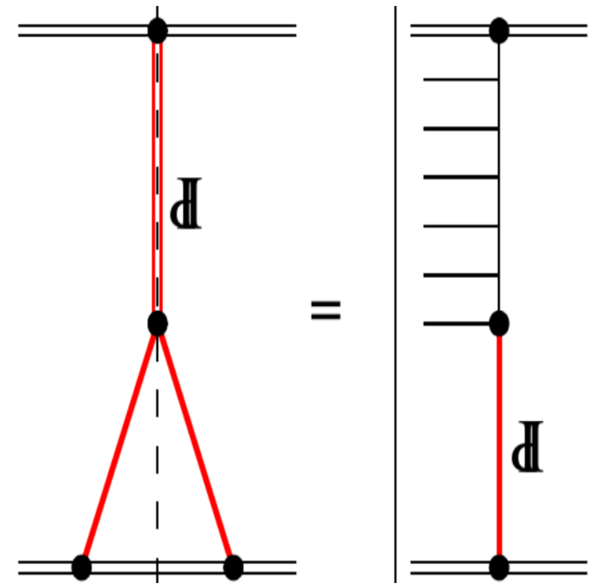

The main problem: to avoid an additional interaction of soft partons which will spoil the coherence.

Survival factor S^2 is the probability to have NO extra interactions

Expected properties of Diffr. Dissoc^n:

a) large impact parameter b_t

at large b_t the optical density is lower leading to a smaller probability of new interaction, i.e. to a larger S^2

b) smaller transverse momenta of partons

(to reach a larger b_t since $\Delta b_t \sim 1/k_t$)

c) small multiplicity

The MODEL

On contrary to DGLAP we consider the evolution in rapidity $y = \ln(1/x)$ (like BFKL) but keeping b_t instead of k_t (however at each x, b_t point the mean $< k_t(x, b_t) >$ is calculated)

Next, the screening corrections are included into the evolution.

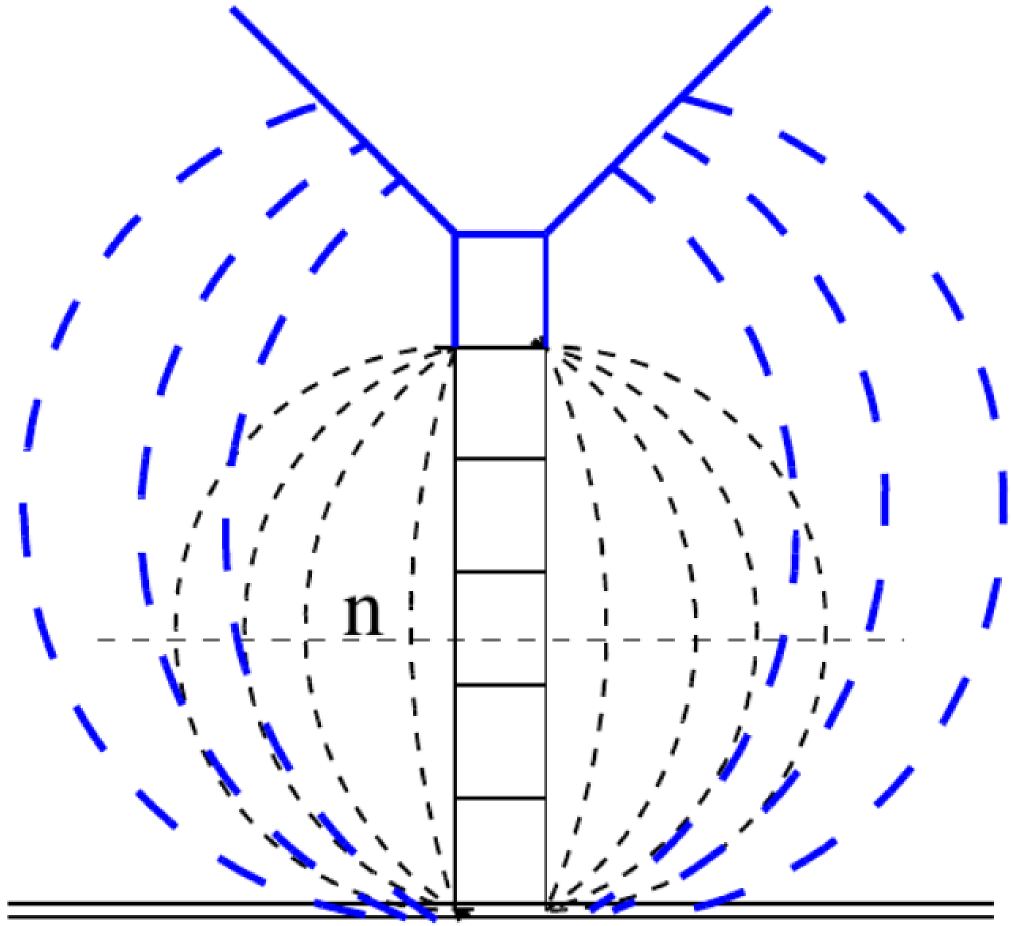

Figure 2: Evolution of the wee parton density in rapidity (momentum fraction) space. The last step of evolution is shown by thick (blue) lines. The dashed curves indicate the eikonal-like absorptive corrections. n is the number of screening Pomerons.

$$\frac{d\Omega(b,y)}{dy} = \Delta\Omega(b,y) \qquad y = \ln(1/x)\,,$$

where we expect that the value of Δ to be close to that ($\omega_{\rm BFKL}$) given by the BFKL [8] intercept $\omega_{\rm BFKL}$. That is accounting for (and re-summing) the next-to-leading logarithm corrections we expect $\Delta \sim 0.15 - 0.2$

Unitarity eq. $2ImA(b,s) = |A|^2 + G_{inel}(b,s)$

$$A(b,s) = i(1 - \exp(-\Omega/2)), \qquad G_{inel} = 1 - \exp(-\Omega)$$

$$S^2(b) = \exp(-\Omega(b)) \qquad at \;\; \Omega \to \infty \quad G \to 1$$

saturation

$$\frac{dG(b,y)}{dy} = \Delta(1 - G(b,y))\,G(b,y)\,.$$

diffusion in the transverse b-plane

$$\Delta b_t \sim 1/k_t \qquad \frac{dP(b)}{db} \;=\; k_t(b)\exp(-bk_t(b))$$

$$\frac{dG(b,y)}{dy} \;=\; (1-G(b,y))\left[\frac{3}{4}\Delta G(b,y) + \frac{1}{4}\Delta\int_0^b db' G(b',y)k_t(b',y)e^{(b'-b)k_t(b',y)}\right]$$

when $G \to 1$ the value of k_t grows

low k_t are absorbed

but not high k_t with $\sigma \sim 1/k_t^2$

$$\frac{dk_t(b,y)}{dy} \;=\; \frac{\Delta}{2}k_t(b,y)G(b,y)$$

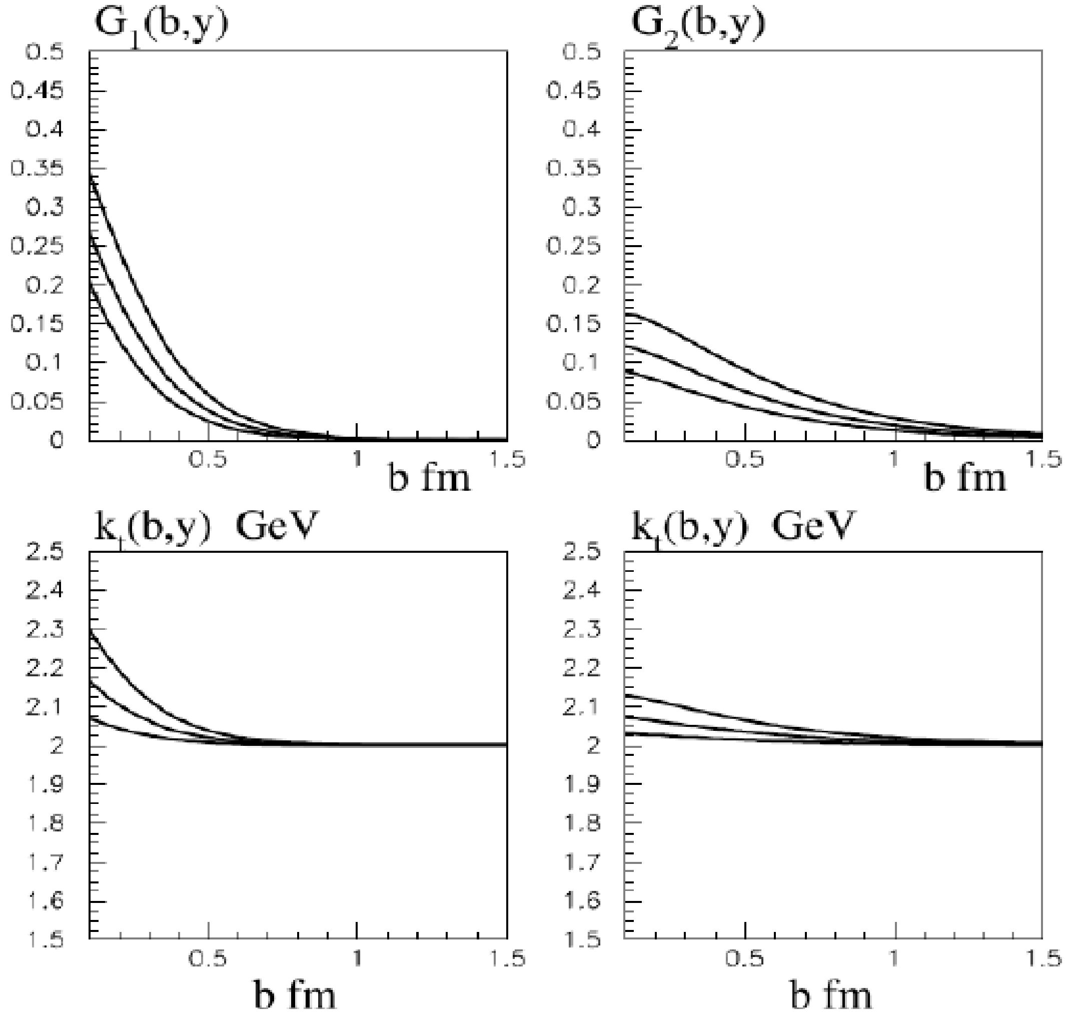

Figure 3: Impact parameter, b, dependence of the parton densities, $G_i(b,y)$ (upper panels) and the characteristic transverse momenta, $k_{ti}(b,y)$ (lower panels) for the two G-W components, $|\phi_1\rangle$ (left) and $|\phi_2\rangle$ (right) at three values of rapidity $y = 9$, 6, 3 – the curves from top to bottom. We use the values of the parameters which have been tuned to describe the total and elastic $p\bar{p}$ and pp cross sections in the S$p\bar{p}$S, Tevatron and the LHC colliders energy range.

$$\Omega_{ij}(b_{ij}) = \int d^2b_1 d^2b_2 G_i(b_1, y_1)\frac{1}{\sigma_0}G_j(b_2, y_2)\delta^{(2)}(\boldsymbol{b}_{ij} - \boldsymbol{b}_1 + \boldsymbol{b}_2)$$

$$\frac{d\sigma_{\rm el}}{dt} = \frac{1}{4\pi}\left|\int d^2b\, e^{i\boldsymbol{q}_t\cdot\boldsymbol{b}}\sum_{i,j}|a_i|^2|a_j|^2\left(1 - e^{-\Omega_{ij}(b)/2}\right)\right|^2$$

$$\mathrm{Re}A(b,s) = \frac{\pi}{2}\frac{\partial\,\mathrm{Im}A(b,s)}{\partial\ln s}$$

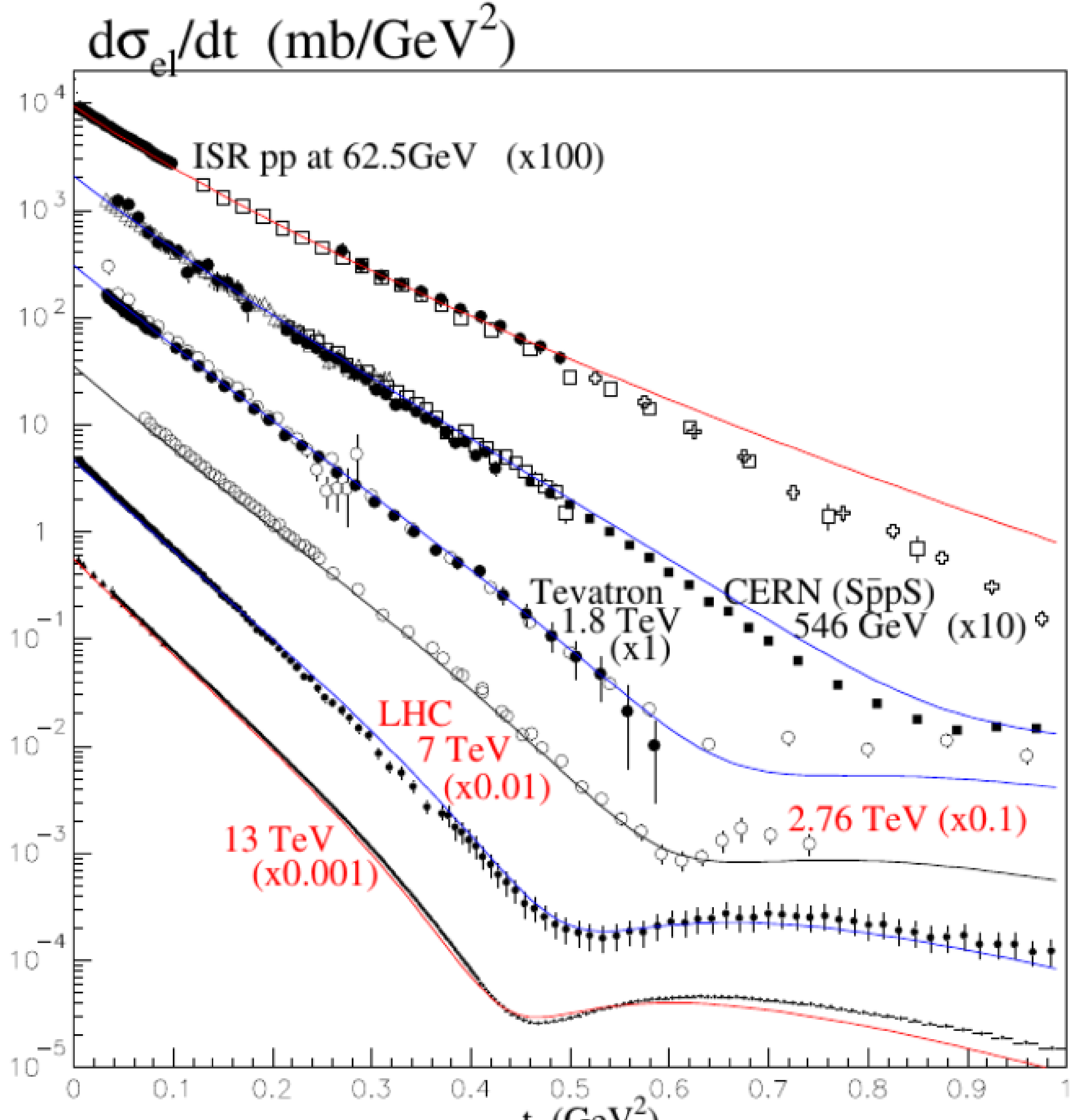

dσel/dt (mb/GeV2)
ISR pp at 62.5GeV (x100)
Tevatron
1.8 TeV
(x1)
CERN (SppS)
546 GeV (x10)
LHC
7 TeV
(x0.01)
2.76 TeV (x0.1)
13 TeV
(x0.001)
-t (GeV2)

Δ	0.17
σ_0 (GeV^{-2})	1.18
k_0 (GeV)	2.2
$\lambda = g_{3P}/g_N$	0.2 (fixed)
f_1	11
d_1 (GeV^{-2})	2.75
c_1 (GeV^2)	0.2
f_2	4.15
d_2 (GeV^{-2})	1.3
c_2 (GeV^2)	0.3

The values of the parameters in the two-channel eikonal fit to elastic pp ($p\bar{p}$) scattering

High-mass diffractive dissociation

cross section takes the form

$$\frac{\xi d\sigma^{\rm SD}}{d\xi} = \frac{d\sigma^{\rm SD}}{dy_1} = \int d^2b_1 \sum_j |a_j|^2 \frac{\lambda G_j(b_1,y_1)}{\sigma_0} d^2b_2$$

$$\left(\sum_i |a_i|^2 (1-\sqrt{1-G_i(b_2,y_2)}) e^{-\Omega_{ij}(\boldsymbol{b}_1+\boldsymbol{b}_2,Y)/2} S_i^{\rm enh}(b_2,y_1)\right)$$

$$\cdot \left(\sum_{i'} |a_{i'}|^2 (1-\sqrt{1-G_{i'}(b_2,y_2)}) e^{-\Omega_{i'j}(\boldsymbol{b}_1+\boldsymbol{b}_2,Y)/2} S_{i'}^{\rm enh}(b_2,y_1)\right)^*$$

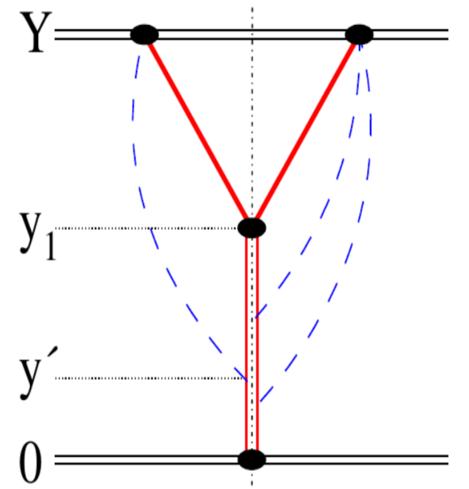

e $y_2 = Y - y_1$ and the 'elastic' amplitude $(1-e^{-\Omega/2})$ generated by the parton cascade (in
pper part of Fig.1), $G_i(b_2,y_2) = 1 - \exp(-\Omega_i(b_2,y_2))$ is written as $(1-\sqrt{1-G})$.

$$S_i^{\rm enh}(b,y_1) = \exp\left(-\int_{1.6}^{y_1} dy' \frac{\lambda}{2} G_i(b,Y-y')\right)$$

$$B_{\rm dis}(t=0) \;=\; \frac{\int d^2b_1 \sum_j |a_j|^2 G_j(b_1,y_1) d^2b_2 b_2^2 \left(\sum_i |a_i|^2 ...\right) \left(\sum_{i'} |a_{i'}|^2 ...\right)^*}{\int d^2b_1 \sum_j |a_j|^2 G_j(b_1,y_1) d^2b_2 \left(\sum_i |a_i|^2 ...\right) \left(\sum_{i'} |a_{i'}|^2 ...\right)^*}\;,$$

e 'dots' denote the corresponding expressions in the second and third lines of (22).

Density of secondaries in LRG events

$$\frac{\xi d\sigma^{\rm SD}}{d\xi dy_s} = \int d^2b_1 d^2b_s \sum_{iji'} |a_i^2||a_{i'}^2||a_j|^2 \frac{g_s G_j(b_1,y_s) G_{sii'}(b_s,y_3)}{\sigma_0} S^{\rm eik}_{ij} S^{\rm eik}_{i'j} S^{\rm enh}_{ii'}(b_s, Y-y_{\rm gap})$$

$$G_{sii'}(b_s,0) = \lambda\left(1-\sqrt{1-G_i(b_s,y_{\rm gap})}\right)\left(1-\sqrt{1-G_{i'}(b_s,y_{\rm gap})}\right)$$

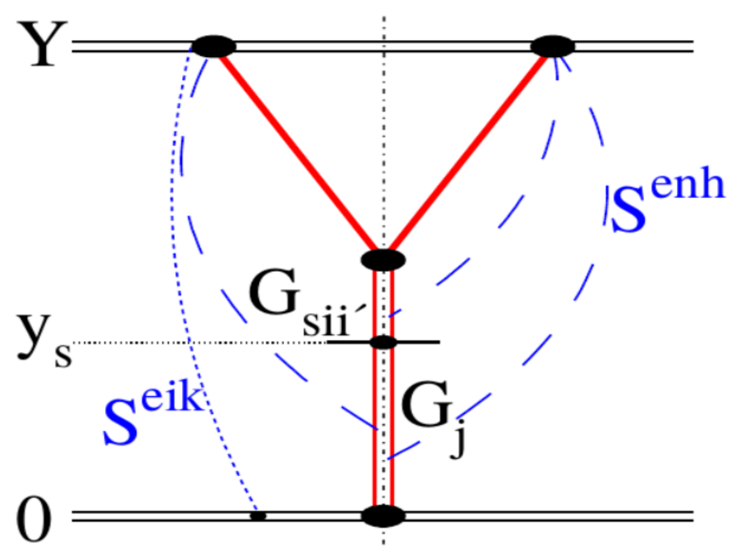

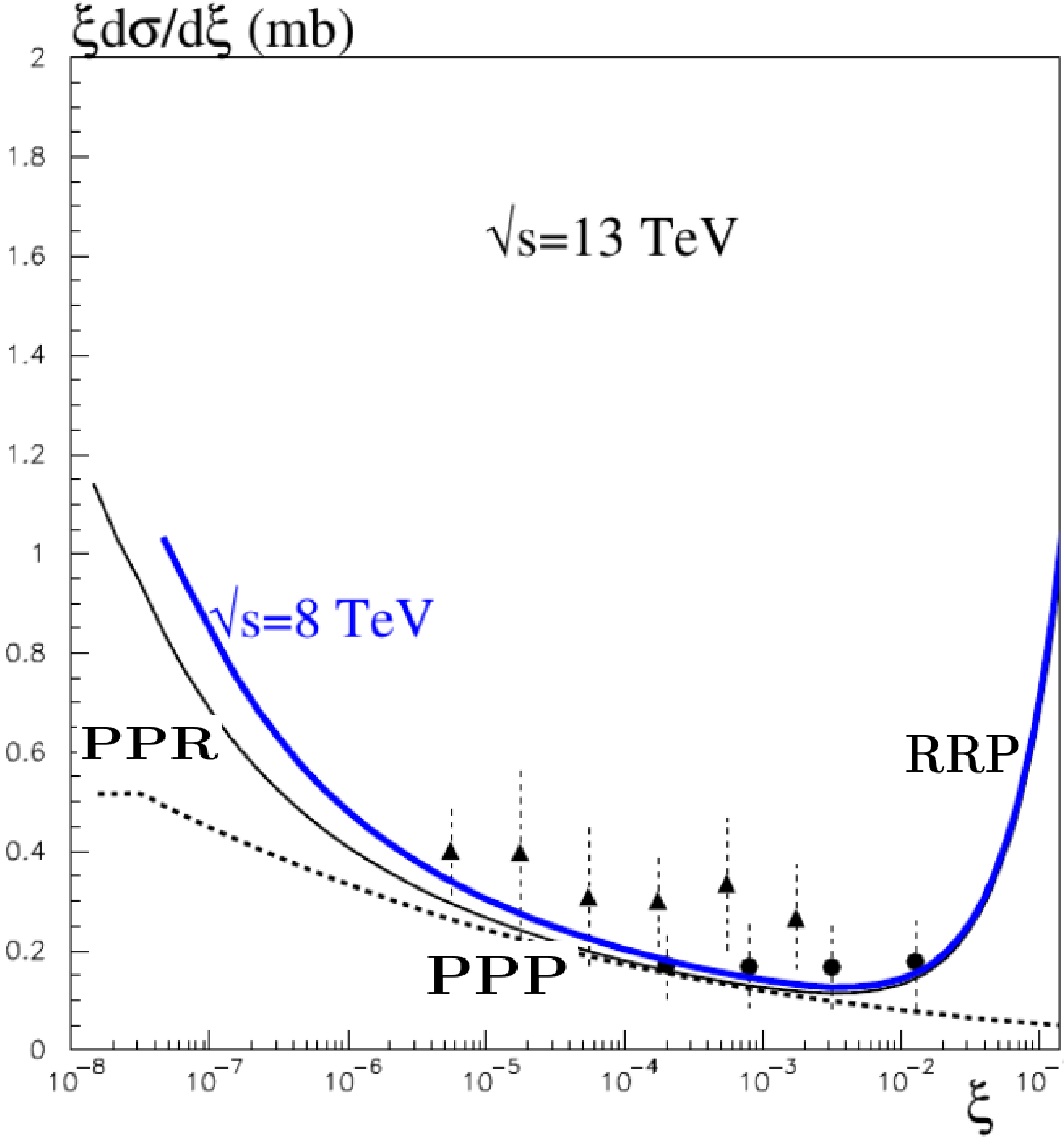

ξdσ/dξ (mb)
√s=13 TeV
√s=8 TeV
PPR
PPP
RRP
ξ
2
1.8
1.6
1.4
1.2
1
0.8
0.6
0.4
0.2
0
10^-8
10^-7
10^-6
10^-5
10^-4
10^-3
10^-2
10^-1

$\xi = 1 - x_L$

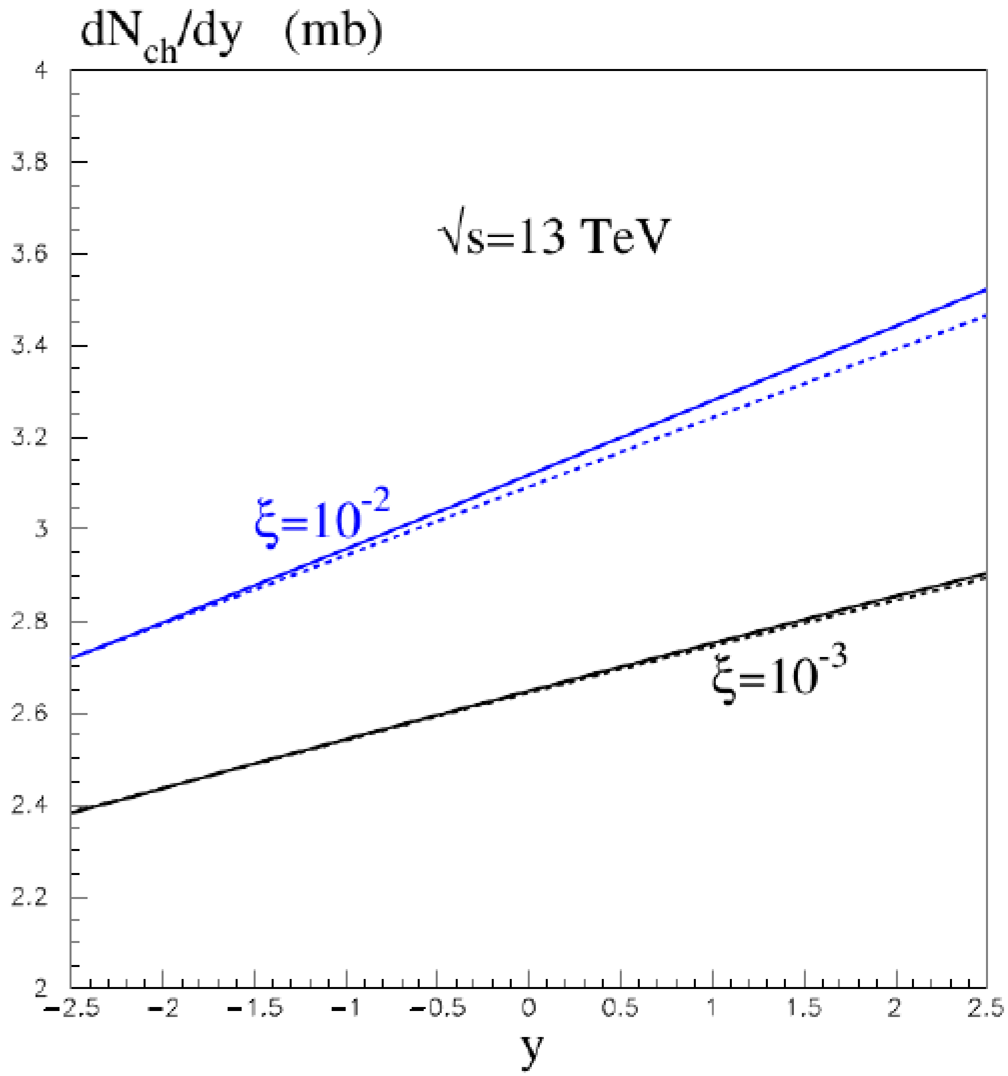

Figure 9: The rapidity dependence of the charged multiplicity observed in the central detector for SD events with $\xi = 0.01$ (blue) and 0.001 (black) at $\sqrt{s} = 13$ TeV. The dashed curves correspond to the pure Pomeron-induced cross section without the secondary Reggeon contribution.

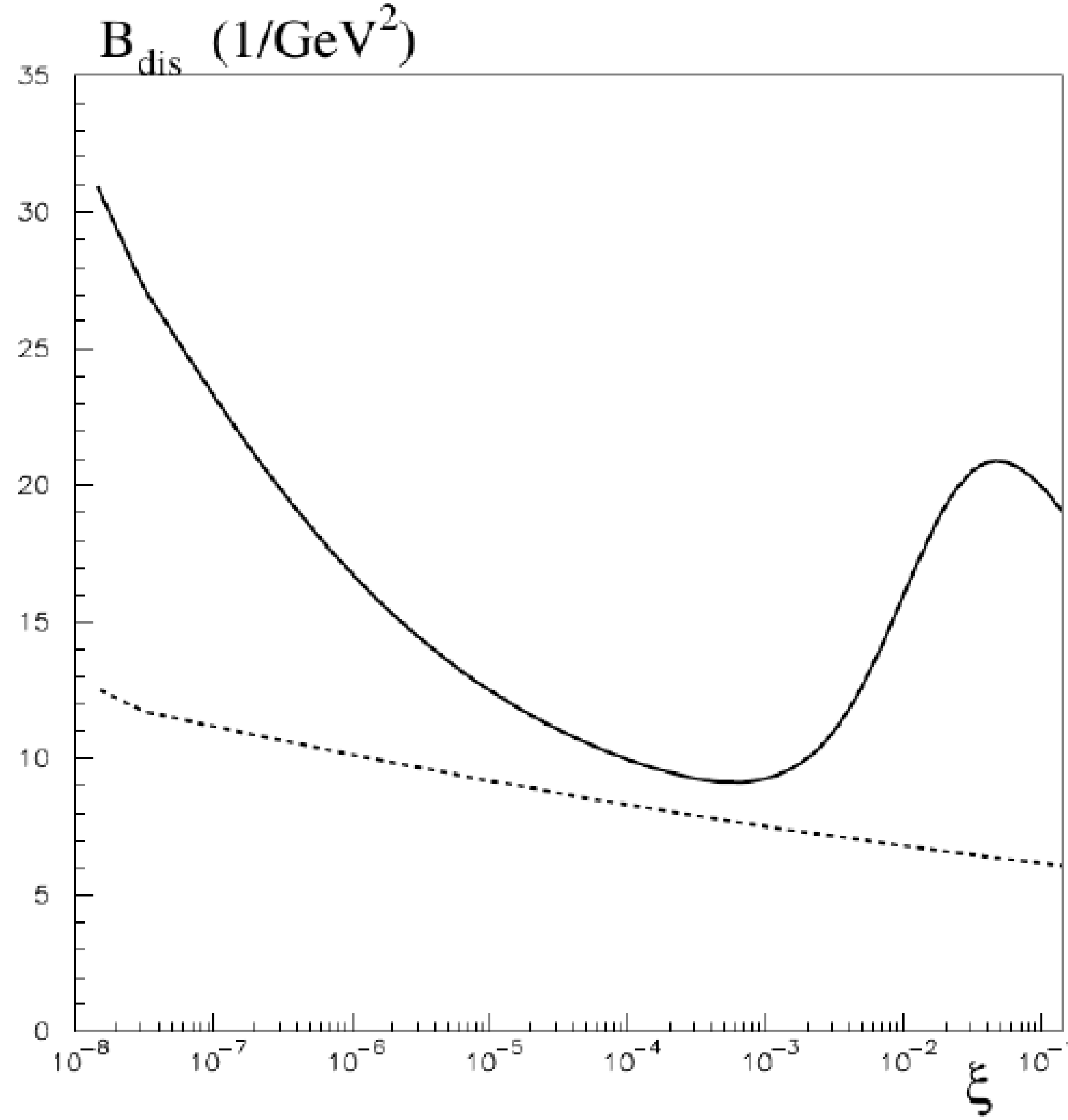

Figure 11: The ξ dependence of the t-slope $B_{\rm dis}(t=0)$ in the single proton dissociation process at $\sqrt{s}=13$ TeV. The dashed curve is the Pomeron component while the continuous curve includes secondary Reggeon contributions. Note that here we show the slope at $t=0$.

Multiplicity distribution

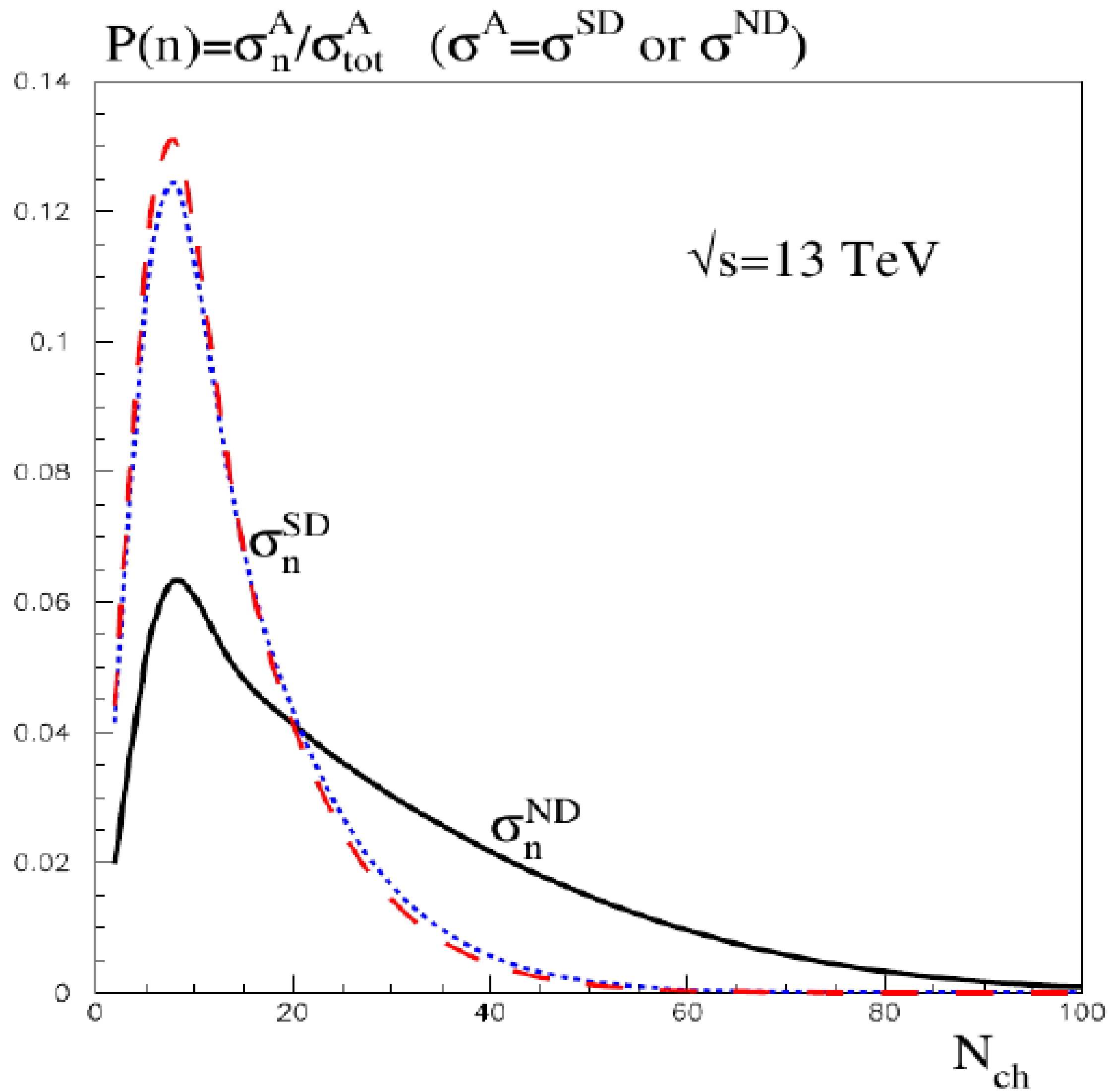

Figure 13: The distribution over the charged hadron multiplicity in non-diffractive (ND) events (continuous curve) and in the case of single proton (SD) dissociation at $\sqrt{s} = 13$ TeV for $\xi = 10^{-3}$ (red long-dashed curve) and $\xi = 10^{-2}$ (blue short-dashed curve).

THANK YOU

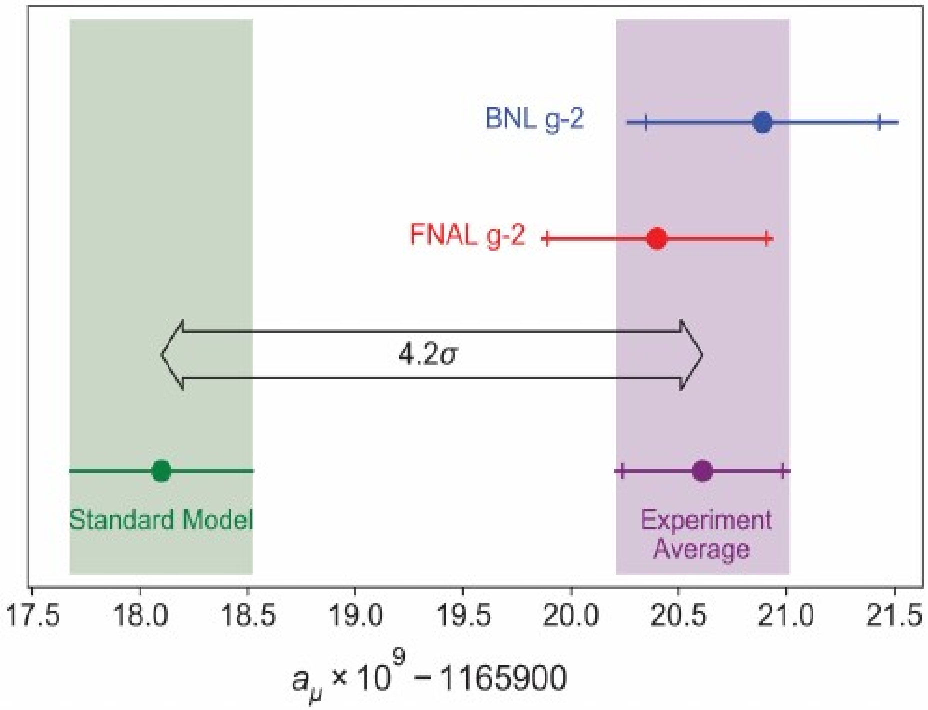
BNL g-2
FNAL g-2
4.2σ
Standard Model
Experiment Average
17.5 18.0 18.5 19.0 19.5 20.0 20.5 21.0 21.5
$a_\mu \times 10^9 - 1165900$

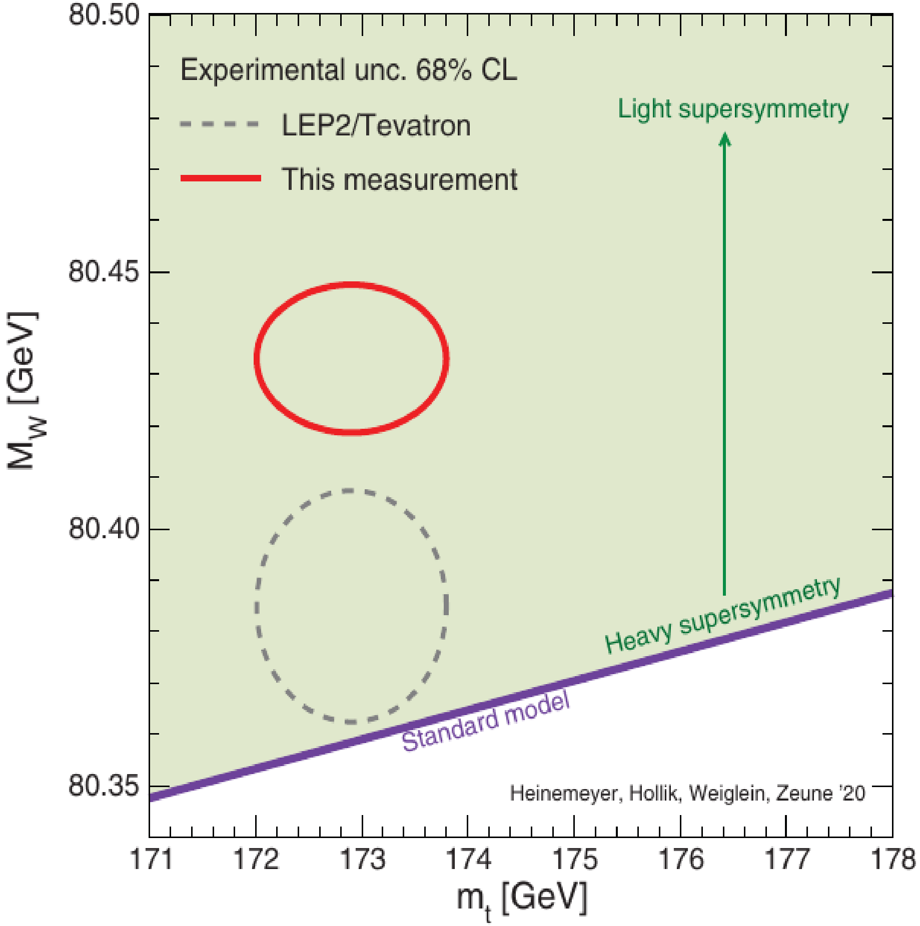

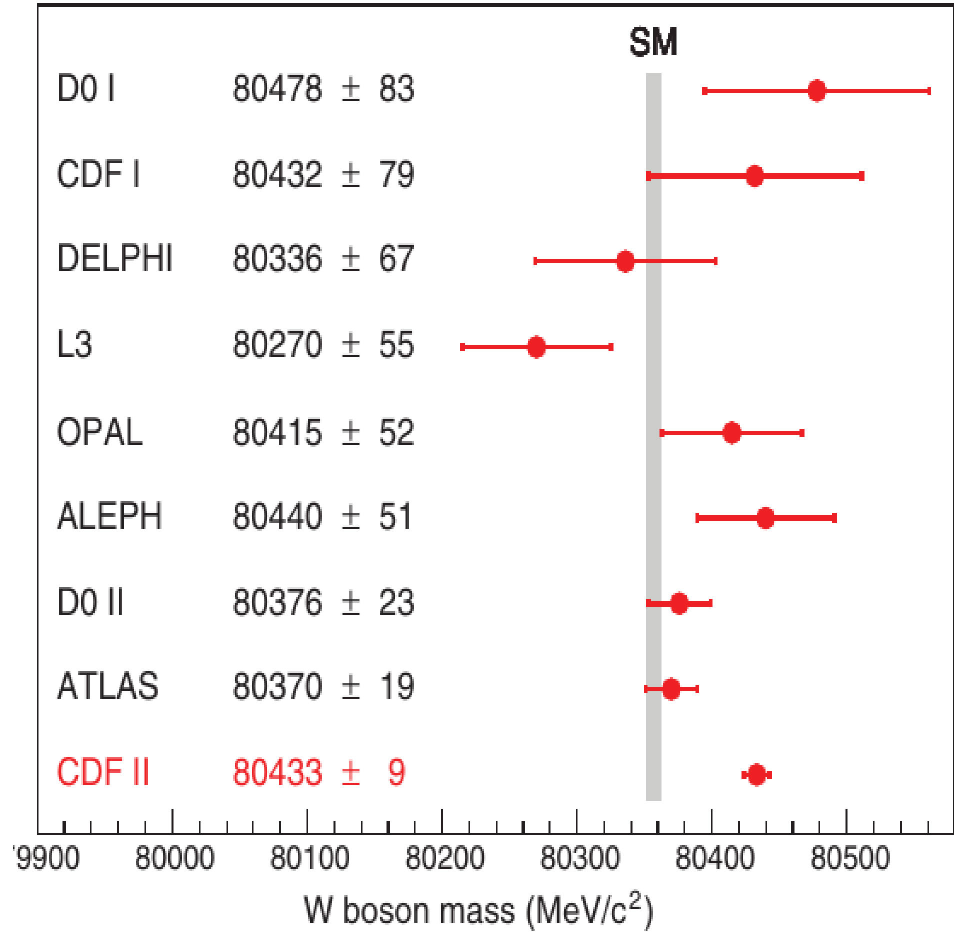

significance of 7.0σ